

# Internal structure in the $B$ meson

Benoît Blossier



CNRS/Laboratoire de Physique Théorique d'Orsay

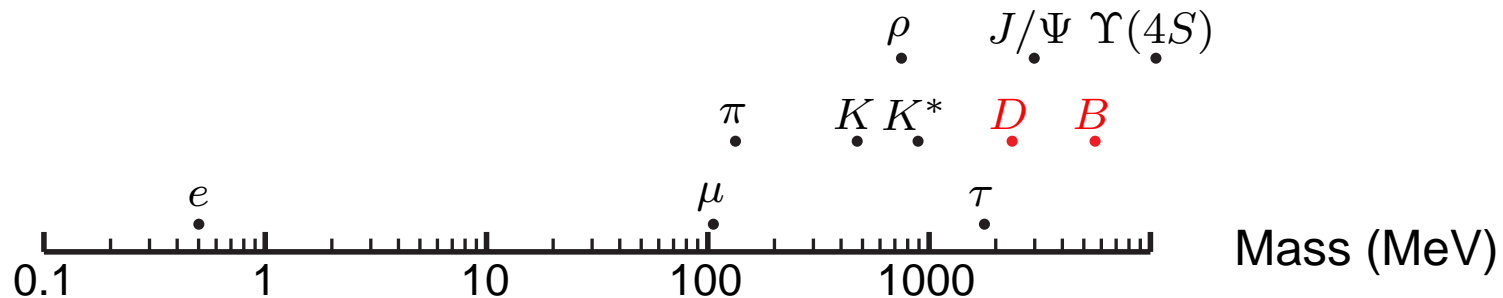
Rencontres de Physique des Particules  
Annecy, 25 – 27 January 2016

- Phenomenology
- Methodology
- Results
- Multihadron states
- Outlook

[In collaboration with Antoine Gérardin (Mainz Univ.)]

# Phenomenology

Non exhaustive spectrum of observed charged leptons and mesons:



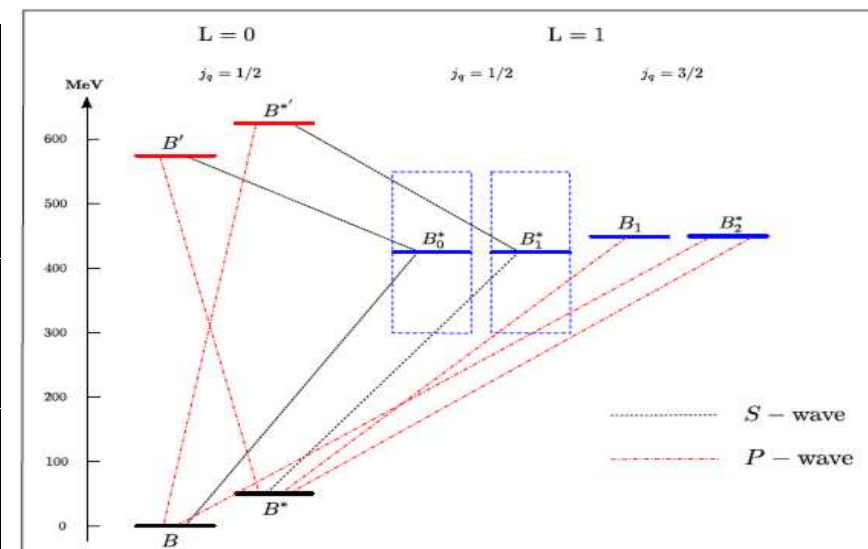
Rich  $B$  and  $D$  mesons phenomenology because of their high number of decay channels

Angular momentum:  $J = \frac{1}{2} \oplus j_l$

Heavy-light mesons are put together in doublets

$H = B, D$ :

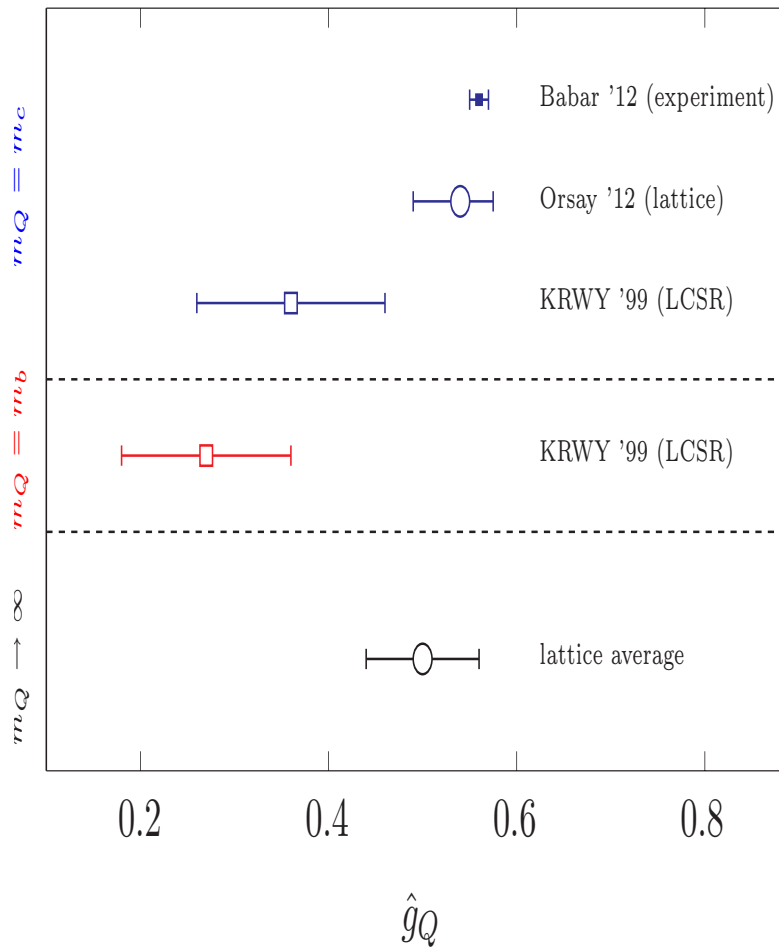
$j_l^P$	$J^P$	orbital excitation	radial excitation
$\frac{1}{2}^-$	$0^-$	$H$	$H'$
	$1^-$	$H^*$	$H^{* \prime}$
$\frac{1}{2}^+$	$0^+$	$H_0^*$	
	$1^+$	$H_1^*$	
$\frac{3}{2}^+$	$1^+$	$H_1$	
	$2^+$	$H_2^*$	



# Interplay between experiment, lattice QCD and analytical methods

$D^* \rightarrow D\pi$ : an ideal process to test analytical computations based on the soft pion theorem:

$$\langle D(p')\pi(q)|D^*(p, \epsilon_\lambda) = g_{D^*D\pi} q \cdot \epsilon_\lambda, \quad g_{H^*H\pi} \equiv \frac{2\sqrt{m_H m_{H^*}} \hat{g}_Q}{f_\pi}$$



Claim: a **negative** radial excitation contribution to the hadronic side of LCSR might explain the discrepancy between  $g_{D^*D\pi}^{\text{exp}}$  and  $g_{D^*D\pi}^{\text{LCSR}}$  [D. Becirevic *et al*, '03].

Without any radial excitation:

$$g_{D^* D \pi} = \frac{f(M^2)}{f_D f_{D^*}}$$

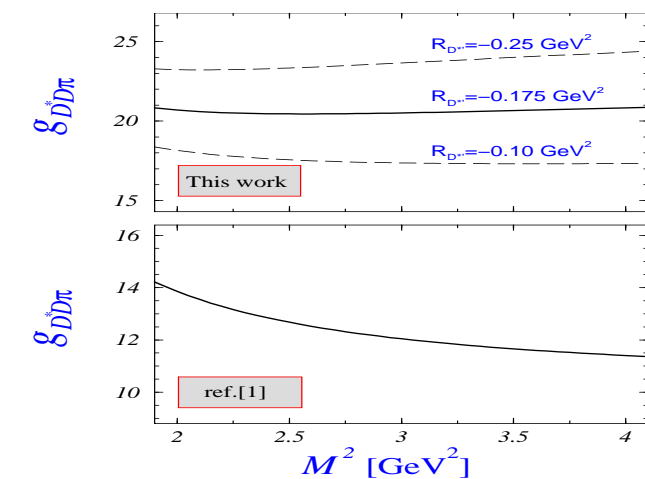
$$f(M^2) = \frac{m_c^2}{m_D^2 m_{D^*}} f_\pi \phi_\pi(1/2) M^2 \exp\left(\frac{m_D^2 + m_{D^*}^2}{2M^2}\right) \left[ e^{-m_c^2/M^2} - e^{-s_0/M^2} \right] + \dots$$

With radial excitation:

$$g_{D^* D \pi} = \frac{1}{f_D f_{D^*}} \left[ f(M^2) - R_{D'} \exp\left(-\frac{m_{D'}^2 - m_D^2}{2M^2}\right) - R_{D^{*\prime}} \exp\left(-\frac{m_{D^{*\prime}}^2 - m_{D^*}^2}{2M^2}\right) \right]$$

$$R_{D'} = \left(\frac{m_{D'}}{m_D}\right)^2 f_{D'} f_{D^*} g_{D^* D' \pi} \quad R_{D^{*\prime}} = \frac{m_{D^{*\prime}}}{m_{D^*}} f_D f_{D^{*\prime}} g_{D^{*\prime} D \pi}$$

Assuming  $m_{D'} = m_{D^{*\prime}}$ ,  $f_{D'} = f_{D^{*\prime}}$  and  $g_{D^* D' \pi} = g_{D^{*\prime} D \pi} = g'$ :  $\frac{R_{D'}}{R_{D^{*\prime}}} = \frac{m_{D^{*\prime}} m_{D^*}}{m_D^2} \frac{f_{D^*}}{f_D}$



$$\begin{aligned} -0.25 \text{ GeV}^2 &< R_{D^{*\prime}} < -0.1 \text{ GeV}^2 \\ \implies 17 &< g_{D^* D \pi} < 25 \end{aligned}$$

Much better stability in Borel window

Our proposal: check on the lattice that statement in the heavy quark limit.

# Methodology

Transition amplitude under interest, with  $q = p' - p$ ,  $\mathcal{A}^\mu = \bar{q}\gamma^\mu\gamma_5 q$  and  $T^{mn\mu} = \langle B^{*(n)}(p', \epsilon_\lambda) | \mathcal{A}^\mu | B^{(m)}(p) \rangle$ :

$$\begin{aligned} T^{mn\mu} &= 2m_{B^{*(n)}} A_0^{mn}(q^2) \frac{\epsilon^{(\lambda)} \cdot q}{q^2} q^\mu + (m_{B^{(m)}} + m_{B^{*(n)}}) A_1^{mn}(q^2) \left( \epsilon^{(\lambda)\mu} - \frac{\epsilon^{(\lambda)} \cdot q}{q^2} q^\mu \right) \\ &+ A_2^{mn}(q^2) \frac{\epsilon^{(\lambda)} \cdot q}{m_{B^{(m)}} + m_{B^{*(n)}}} \left[ (p + p')^\mu + \frac{m_{B^{(m)}}^2 - m_{B^{*(n)}}^2}{q^2} q^\mu \right] \end{aligned}$$

With  $q = (q^0, 0, 0, q_z)$  and  $\langle B^{(m)}(p) \pi(q) | B^{*(n)}(p', \epsilon_\lambda) \rangle = \epsilon_\lambda \cdot q g_{B^{*(n)} B^{(m)} \pi}$ :

$$g_{B^{*(n)} B^{(m)} \pi} f_\pi = \langle B^{*(n)}(p', \epsilon_\lambda) | q_0 \mathcal{A}^0 - q_z \mathcal{A}^3 | B^{(m)}(p) \rangle = 2m_{B^{*(n)}} A_0^{mn}(q^2 = 0)$$

$$2m_{B^{*(n)}} A_0^{mn}(0) = (m_{B^{(m)}} + m_{B^{*(n)}}) A_1^{mn}(0) + (m_{B^{(m)}} - m_{B^{*(n)}}) A_2^{mn}(0)$$

HQET normalisation of states:  $|B\rangle = \sqrt{2m_B} |B\rangle_{\text{HQET}}$ ,  $\langle B(p) | B(p') \rangle = 2E(p) \delta^3(\vec{p} - \vec{p}')$ :

$$\langle B^{*(n)}(p', \epsilon_\lambda) | q_0 \mathcal{A}^0 - q_z \mathcal{A}^3 | B^{(m)}(p) \rangle_{\text{HQET}} = A_0^{mn}(0)$$

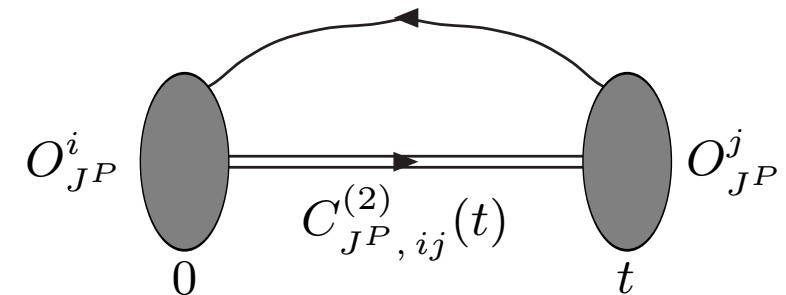
Back to the  $x$  space:

$$A_0^{mn}(q^2 = 0) = q_0 \int e^{i\vec{q} \cdot \vec{r}} \langle B^{*(n)} | \mathcal{A}^0(r) | B^{(m)}(p) \rangle - q_z \int e^{i\vec{q} \cdot \vec{r}} \langle B^{*(n)} | \mathcal{A}^3(r) | B^{(m)}(p) \rangle$$

Axial density distributions:  $f_{\gamma_\mu \gamma_5}^{mn}(r) = \sum_\lambda \langle H^{(*)(n)}(p', \epsilon_\lambda) | [\bar{\psi}_l \gamma_\mu \gamma_5 \psi](r) | H^{(m)}(p) \rangle$

Variational method: define an operator  $O_{JP}^n$  weakly coupled to other states than  $|n\rangle$

[C. Michael, '85] [M. Lüscher and U. Wolff, '90] [B. B. et al, '09]



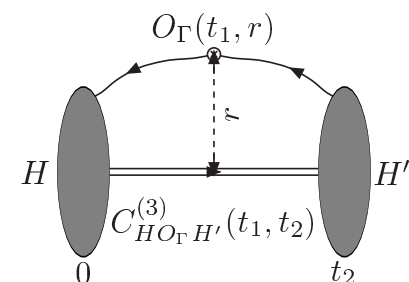
– Compute an  $N \times N$  **matrix of correlators**

$$C_{P(V), ij}^{(2)}(t) = \sum_{\vec{x}, \vec{y}} \langle \Omega | \mathcal{T}[O_{P(V)}^i(\vec{x}, t) O_{P(V)}^j(\vec{y}, 0)] | \Omega \rangle$$

$$O_{P(V)}^i(\vec{x}, t) = \sum_{\vec{z}} \bar{q}(\vec{x}, t) [\Gamma \times \Phi(|\vec{x} - \vec{z}|)]_{P(V)}^i q(\vec{z}, t)$$

– Solve the **generalised eigenvalue problem**

$$C_{P(V)}^{(2)}(t) v_{P(V), n}(t, t_0) = \lambda_{P(V), n}(t, t_0) C_{P(V)}^{(2)}(t_0) v_{P(V), n}(t, t_0), \quad \lambda_n(t, t_0) \sim e^{-E_n(t-t_0)}$$



Two ratio methods, GEVP and sGEVP [J. Bulava et al, '11], to extract  $f_{\gamma_\mu \gamma_5}^{mn}(r)$ :

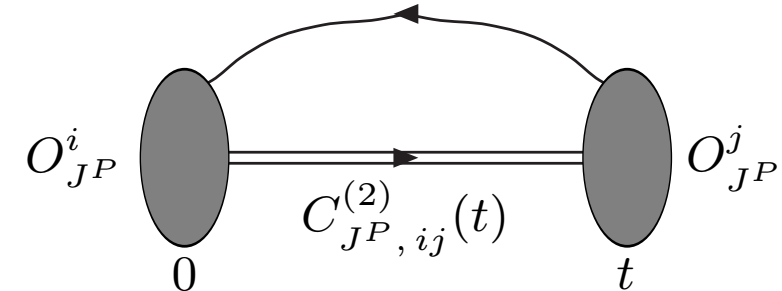
$$\begin{aligned} \mathcal{R}_{mn}^{\text{GEVP}}(t, t_1; \vec{r}) &= \left( v_m(t_2, t_0), C_{\gamma_\mu \gamma_5}^{(3)}(t_1 + t_2, t_1; \vec{r}) w_n(t_1, t_0) \right) G_n(t_1) G'_m(t_2) \\ &= f_{\gamma_\mu \gamma_5}^{(mn)}(\vec{r}) + \mathcal{O}\left(e^{-\Delta_{N+1,m} t_2}, e^{-\Delta_{N+1,n} t_1}\right), \quad \Delta_{nm} = E_n - E_m \end{aligned}$$

$$G_n(t) = \frac{\tilde{\lambda}_n(t_0+1, t_0)^{-t/2}}{\left( w_n(t_1, t_0), C_V^{(2)}(t_1) w_n(t_1, t_0) \right)^{1/2}}, \quad G'_n(t) = \frac{\lambda_n(t_0+1, t_0)^{-t/2}}{\left( v_n(t_1, t_0), C_P^{(2)}(t_1) v_n(t_1, t_0) \right)^{1/2}}$$

Axial density distributions:  $f_{\gamma_\mu \gamma_5}^{mn}(r) = \sum_\lambda \langle H^{(*)(n)}(p', \epsilon_\lambda) | [\bar{\psi}_l \gamma_\mu \gamma_5 \psi](r) | H^{(m)}(p) \rangle$

Variational method: define an operator  $O_{JP}^n$  weakly coupled to other states than  $|n\rangle$

[C. Michael, '85] [M. Lüscher and U. Wolff, '90] [B. B. et al, '09]



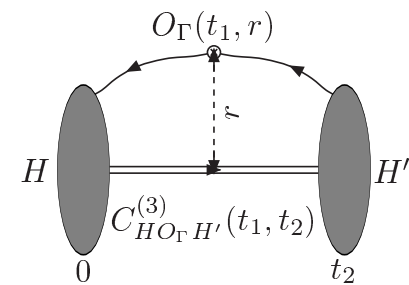
– Compute an  $N \times N$  **matrix of correlators**

$$C_{P(V), ij}^{(2)}(t) = \sum_{\vec{x}, \vec{y}} \langle \Omega | \mathcal{T}[O_{P(V)}^i(\vec{x}, t) O_{P(V)}^j(\vec{y}, 0)] | \Omega \rangle$$

$$O_{P(V)}^i(\vec{x}, t) = \sum_{\vec{z}} \bar{q}(\vec{x}, t) [\Gamma \times \Phi(|\vec{x} - \vec{z}|)]_{P(V)}^i q(\vec{z}, t)$$

– Solve the **generalised eigenvalue problem**

$$C_{P(V)}^{(2)}(t) v_{P(V), n}(t, t_0) = \lambda_{P(V), n}(t, t_0) C_{P(V)}^{(2)}(t_0) v_{P(V), n}(t, t_0), \quad \lambda_n(t, t_0) \sim e^{-E_n(t-t_0)}$$



Two ratio methods, GEVP and sGEVP [J. Bulava et al, '11], to extract  $f_{\gamma_\mu \gamma_5}^{mn}(r)$ :

$$\mathcal{R}_{mn}^{\text{sGEVP}}(t, t_0; \vec{r}) = -\partial_t \left( \frac{|(v_m(t, t_0), K'(t, t_0; \vec{r}) w_n(t, t_0))| e^{\Sigma_{mn}(t_0, t_0)t_0/2}}{\sqrt{[v_m(t, t_0), C_P^{(2)}(t_0)v_m(t, t_0)][w_n(t, t_0), C_V^{(2)}(t_0)w_n(t, t_0)]}} \right)$$

$$\mathcal{R}_{mn}^{\text{sGEVP}}(t, t_0; \vec{r}) = \underbrace{f_{\gamma_\mu \gamma_5}^{(mn)}(\vec{r}) + \mathcal{O}\left(t e^{-\Delta_{N+1,n} t}\right)}_{n > m}, \quad \underbrace{f_{\gamma_\mu \gamma_5}^{(mn)}(\vec{r}) + \mathcal{O}\left(e^{-\Delta_{N+1,m} t}\right)}_{n < m} \quad (1)$$

$$\Sigma_{mn}(t, t_0) = E_n(t, t_0) - E_m(t, t_0), \quad K'(t, t_0, \vec{r}) = K(t, t_0; \vec{r}) / \tilde{\lambda}_n(t, t_0) - K(t_0, t_0; \vec{r}),$$

$$K(t, t_0; \vec{r}) = \sum_{t_1} e^{-(t-t_1)\Sigma_{mn}(t, t_0)} C_{\gamma_\mu \gamma_5}^{(3)}(t, t_1; \vec{r})$$

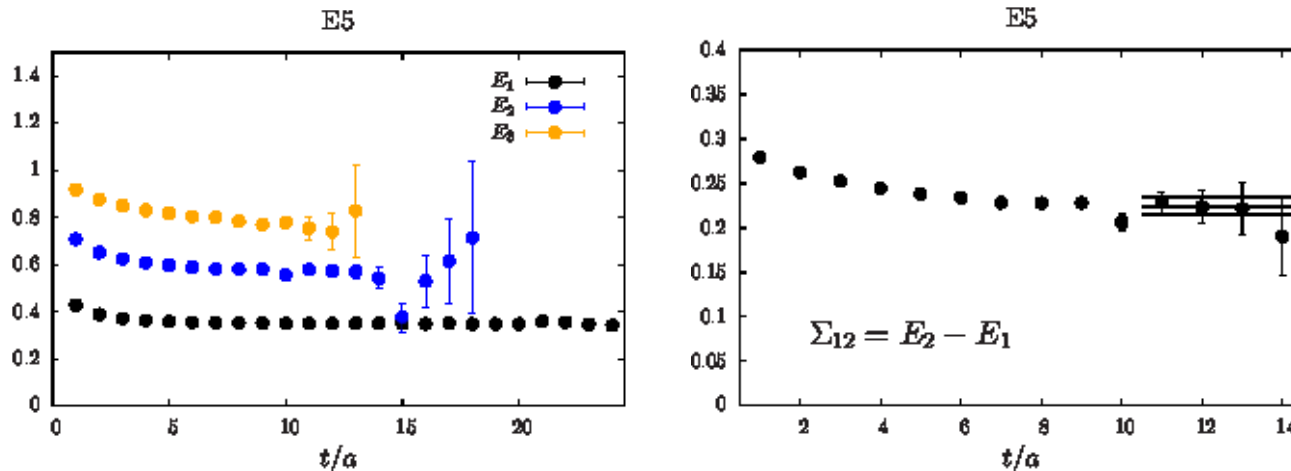
# Results

Lattice set-up:  $\mathcal{O}(a)$  improved Wilson-Clover (light quark), HYP2 (static quark)

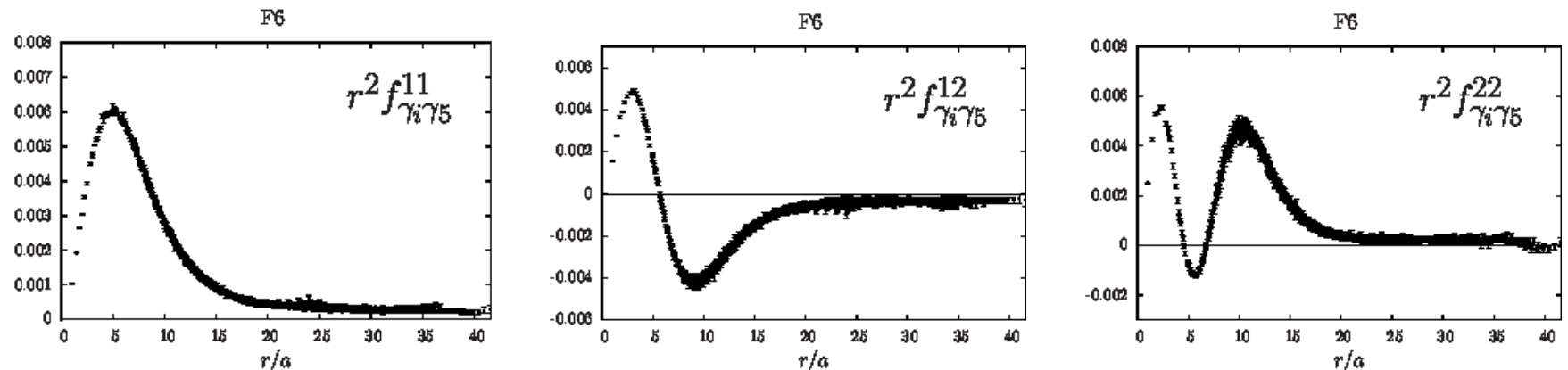
CLS  
based

lattice	$\beta$	$L^3 \times T$	$a[\text{fm}]$	$m_\pi[\text{MeV}]$	$Lm_\pi$
A5	5.2	$32^3 \times 64$	0.075	330	4
B6		$48^3 \times 96$		280	5.2
D5	5.3	$24^3 \times 48$	0.065	450	3.6
E5		$32^3 \times 64$		440	4.7
F6		$48^3 \times 96$		310	5
N6	5.5	$48^3 \times 96$	0.048	340	4
Q1	6.2885	$24^3 \times 48$	0.06	-	-
Q2	6.2885	$32^3 \times 64$	0.06	-	-

Basis of interpolating fields ( $4 \times 4$  matrix of correlators) large enough to well isolate the ground state and the first excited state.



## Spatial component of the axial density distribution: data can be exploited

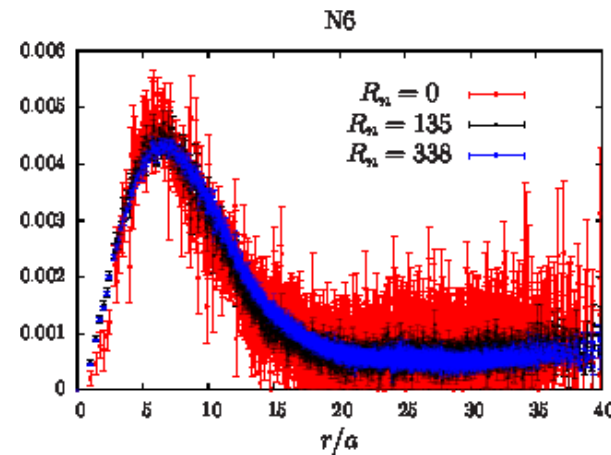


$f_{\gamma_i \gamma_5}^{11}(r)$ : positive everywhere;  $f_{\gamma_i \gamma_5}^{12}(r)$ : there is a node;  $f_{\gamma_i \gamma_5}^{22}(r)$ : almost positive, negative part interpreted by relativistic effects

Issues: densities do not vanish at large  $r$ , curves are not smooth in  $r$

Need to investigate several sources of systematics

- Contamination from excited states, test different interpolating fields



- Cut-off effects

Smoothen the fishbone structure [C. Roiesnel and F. de Soto, '07; B. B. et al, '11].

Different lattice points  $(r_1, r_2, r_3)$  can have the same  $r^2$  but different  $r^{[4]} \equiv \sum_{i=1}^3 r_i^4$ .

Preferred fit form:  $a^3 f_\alpha(r^2, r^{[4]}, r^{[6]}) = a^3 f_\alpha(r^2, 0, 0) + A \times \frac{a^2 r^{[4]}}{r^6} + B \times \frac{a^2 r^{[6]}}{r^8}$ ,  $f_\alpha(r^2, 0, 0)$ ,  $A$  and  $B$  are fit parameters. Small impact of cut-off effects at large  $r$ .

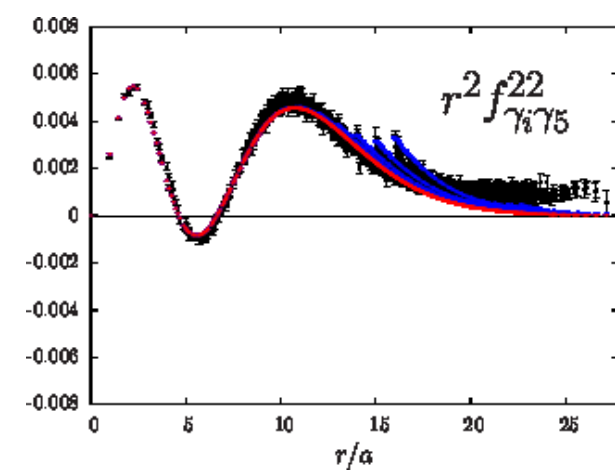
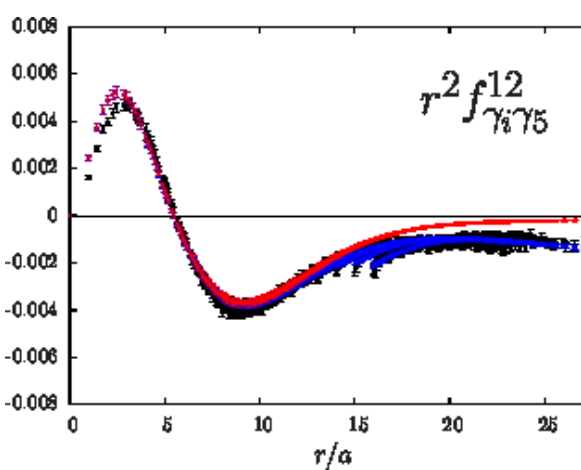
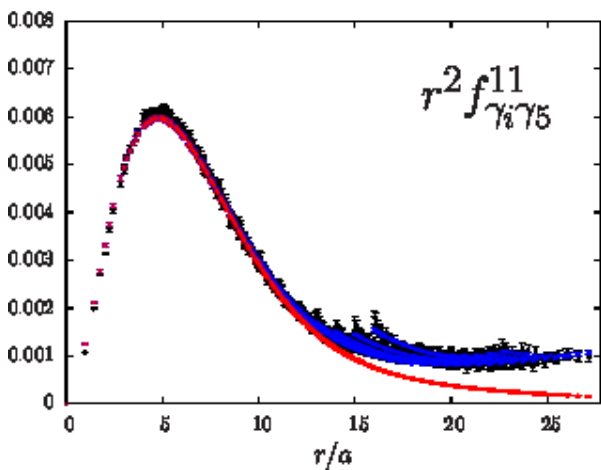
- Finite volume effects

With periodic boundary conditions in space,  $a^3 f_{\gamma_i \gamma_5}^{\text{lat}}(\vec{r}) = \sum_{\vec{n}} a^3 \tilde{f}_{\gamma_i \gamma_5}(\vec{r} + \vec{n}L)$ ,  $n_i \in \mathbb{Z}$ .

$\tilde{f}_{\gamma_i \gamma_5}(\vec{r})$  can still differ from  $f_{\gamma_i \gamma_5}(\vec{r})$  due to interactions among periodic images.

Assumptions: no interaction among images,  $n_i = 0, 1$  taken into account.

Fit form:  $f_{\gamma_i \gamma_5}^{(mn)}(\vec{r}) = P_{mn}(r) \left( \frac{r}{a_0} \right)^\epsilon \exp(-r/r_0)$ ,  $P_{mn}$  is a polynomial.



Distributions vanish at large  $r$ ; good fit, nothing relevant if terms like  $\exp(-(r/r_1)^\beta)$  added

- Cut-off effects

Smoothen the fishbone structure [C. Roiesnel and F. de Soto, '07; B. B. et al, '11].

Different lattice points  $(r_1, r_2, r_3)$  can have the same  $r^2$  but different  $r^{[4]} \equiv \sum_{i=1}^3 r_i^4$ .

Preferred fit form:  $a^3 f_\alpha(r^2, r^{[4]}, r^{[6]}) = a^3 f_\alpha(r^2, 0, 0) + A \times \frac{a^2 r^{[4]}}{r^6} + B \times \frac{a^2 r^{[6]}}{r^8}$ ,  $f_\alpha(r^2, 0, 0)$ ,  $A$  and  $B$  are fit parameters. Small impact of cut-off effects at large  $r$ .

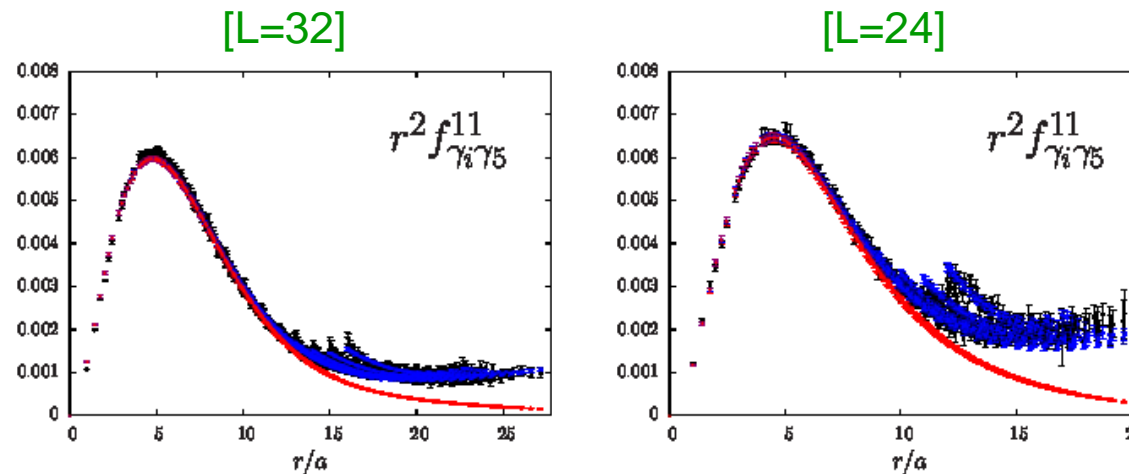
- Finite volume effects

With periodic boundary conditions in space,  $a^3 f_{\gamma_i \gamma_5}^{\text{lat}}(\vec{r}) = \sum_{\vec{n}} a^3 \tilde{f}_{\gamma_i \gamma_5}(\vec{r} + \vec{n}L)$ ,  $n_i \in \mathbb{Z}$ .

$\tilde{f}_{\gamma_i \gamma_5}(\vec{r})$  can still differ from  $f_{\gamma_i \gamma_5}(\vec{r})$  due to interactions among periodic images.

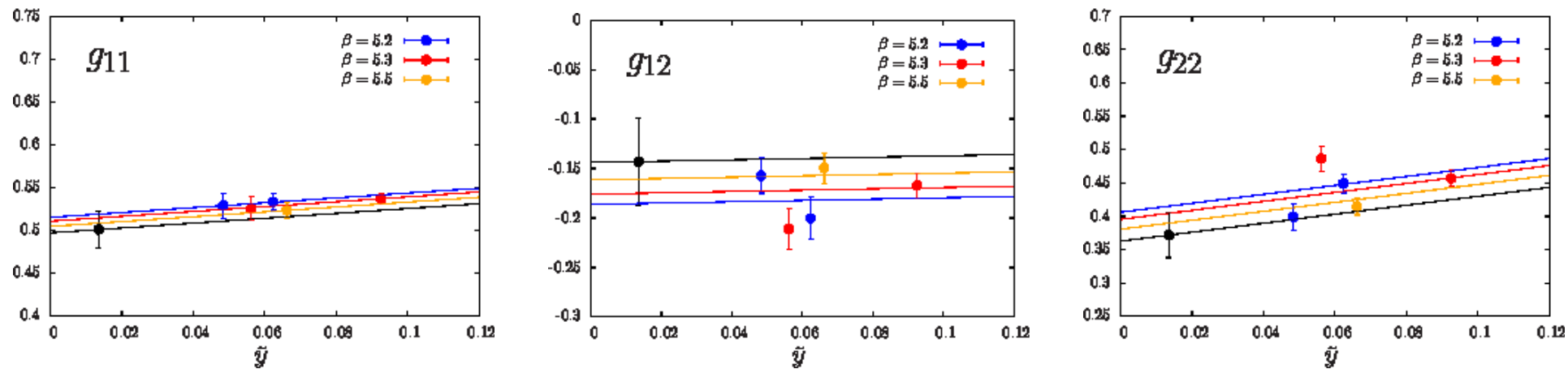
Assumptions: no interaction among images,  $n_i = 0, 1$  taken into account.

Fit form:  $f_{\gamma_i \gamma_5}^{(mn)}(\vec{r}) = P_{mn}(r) \left( \frac{r}{a_0} \right)^\epsilon \exp(-r/r_0)$ ,  $P_{mn}$  is a polynomial.

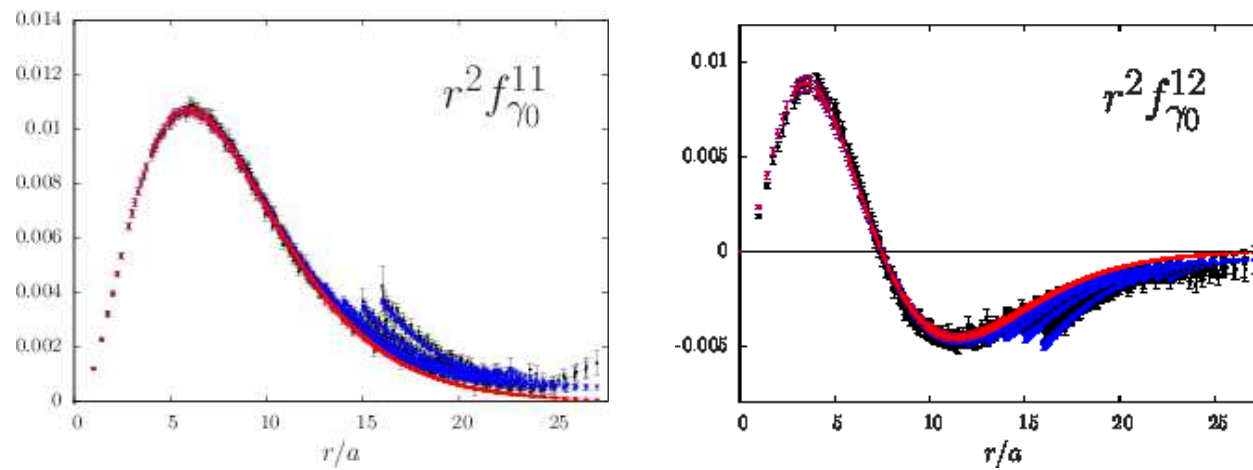


Fit parameters of data ( $L = 32$ ) describe also data ( $L = 24$ ).

Summation over  $r$  of  $f_{\gamma_i \gamma_5}^{mn}(r)$  to get  $g_{mn}$ . After renormalisation, a continuum and chiral extrapolation is possible:  $\bar{g}_{nm}(a, m_\pi) = \bar{g}_{nm} + C_1 a^2 + C_2 m_\pi^2 / (8\pi f_\pi^2)$

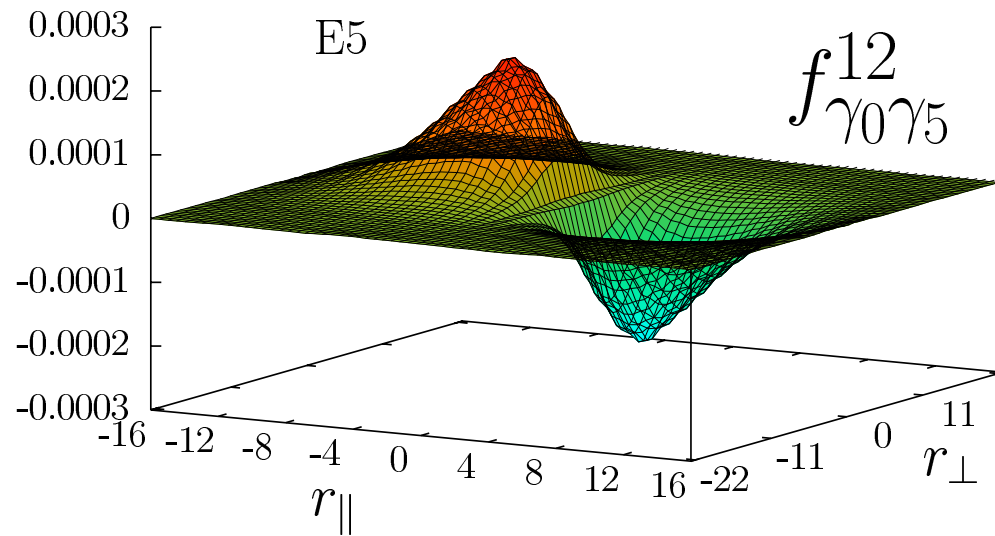


Technique employed also for the charge density distribution  $f_{\gamma_0}^{mn}(r)$



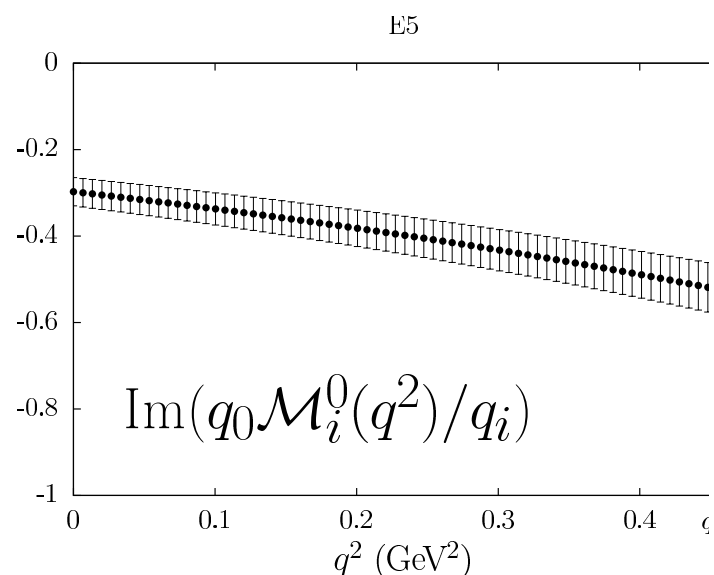
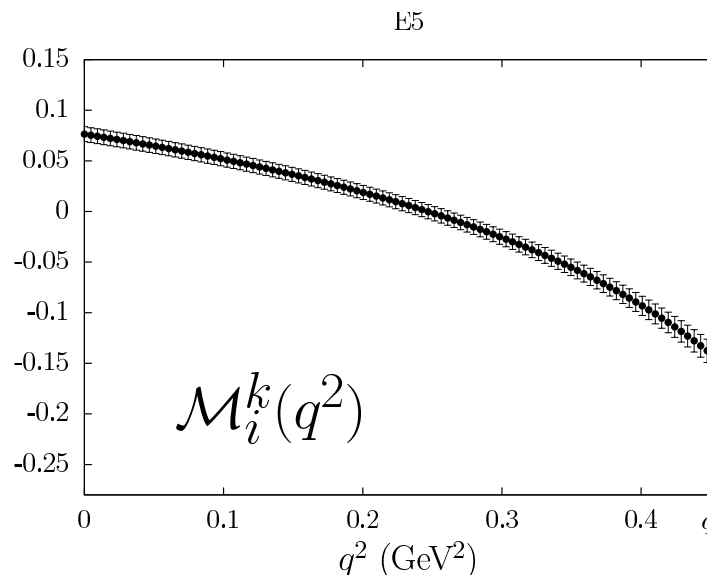
Including  $Z_V$ ,  $\int dr r^2 f_{\gamma_0}^{11}(r)$  compatible with 1.  $\int dr r^2 f_{\gamma_0}^{12}(r)$  compatible with 0.

# Time component of the axial density distribution: systematics more tricky to estimate

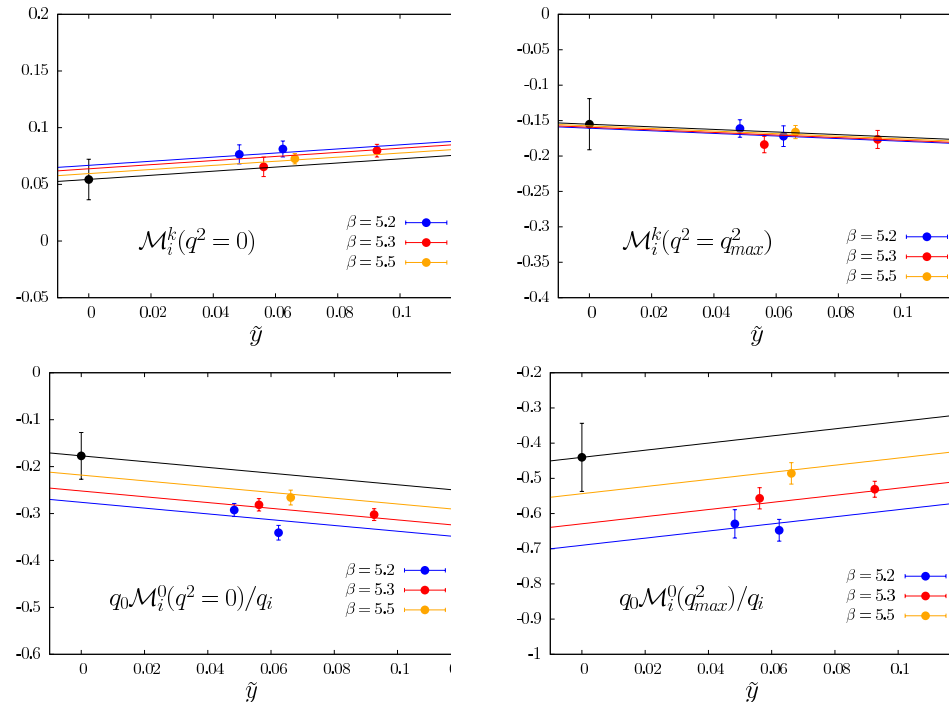


Distribution odd in  $r_{\parallel}$ , along the vector meson polarisation

Matrix elements obtained at  $q$  after a Fourier transform of the distributions to get  $g_{B^* \gamma B\pi}$



# Lattice results and comparison with quark models (*à la* Bakamjian-Thomas/Godfrey-Isgur, Dirac) [A. Le Yaouanc, private communication]



	$q^2 = 0$	$q^2 = q_{\max}^2$
$q_k \mathcal{M}_i^k(q^2)/q_i$ (lattice)	0.05(2)	-0.154(8)
$q_k \mathcal{M}^k(q^2)/q_i$ (BT, GI)	0.103	-0.05
$ q_k \mathcal{M}^k(q^2)/q_i $ (Dirac)	0.223	0.056
$q_0 \mathcal{M}_i^0(q^2)/q_i$ (lattice)	-0.18(5)	-0.45(10)
$q_0 \mathcal{M}^0(q^2)/q_i$ (BT, GI)	-0.467	-0.322
$ q_0 \mathcal{M}^0(q^2)/q_i $ (Dirac)	0.38	0.285

Accidental stability of  $A_0^{12}$  at  $q_{\max}^2$  (-0.154(8)) and 0 (-0.13(5) [preliminary]): confirmation of the hypothesis  $g_{B^* B \pi} < 0$ .

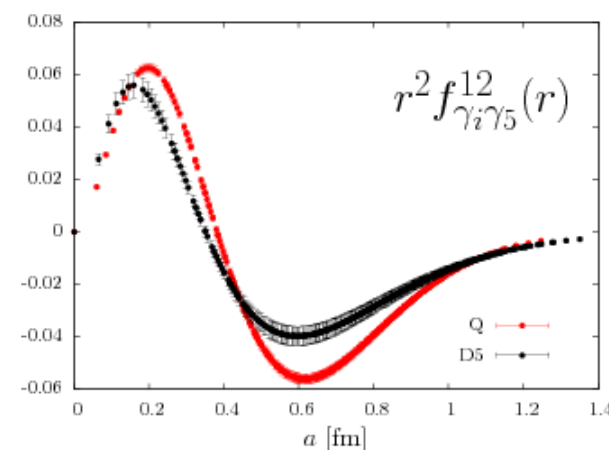
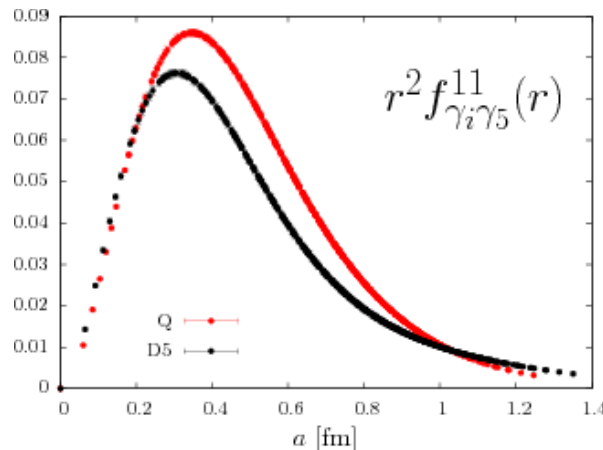
# Multihadron states

A possible unpleasant systematics of our results is an uncontrolled mixing between radial excitations ( $B^{*}'$ ) and multihadron states ( $B_1^*\pi$  in  $S$  wave) close to threshold.

$$\delta = m_{B_1^*} - m_B$$

lattice	$a\Sigma_{12}$	$a\delta + am_\pi$
A5	0.253(7)	0.281(4)
B6	0.235(8)	0.248(4)
E5	0.225(10)	0.278(6)
F6	0.213(11)	0.233(3)
N6	0.166(9)	0.176(3)

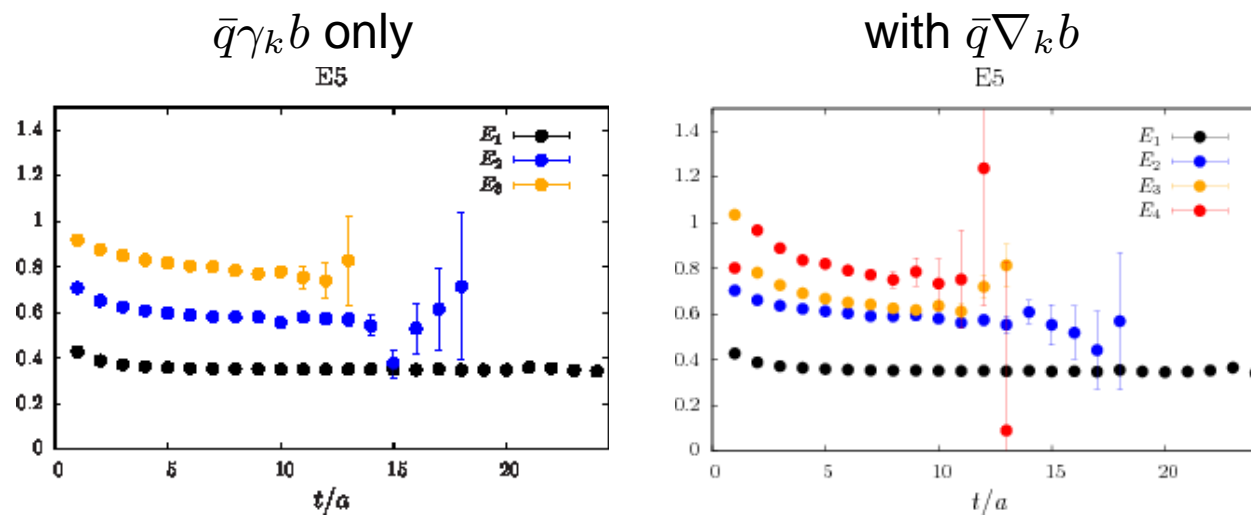
Comparison with quenched data: behaviour of  $f_{\gamma_i\gamma_5}^{11}$  and  $f_{\gamma_i\gamma_5}^{12}$  similar



At  $N_f = 2$ , position of the node of  $f_{\gamma_i \gamma_5}^{12}$  weakly dependent of  $m_\pi$  in the range we have considered

lattice	$m_\pi$ [MeV]	$r_n^{12}$ [fm]
A5	330	0.371(6)
B6	280	0.369(6)
E5	440	0.369(4)
F6	330	0.371(3)
N6	340	0.358(4)

Change observed when  $\bar{q}\nabla_k b$  is included in addition to  $\bar{q}\gamma_k b$  to couple to  $B^{*}'$



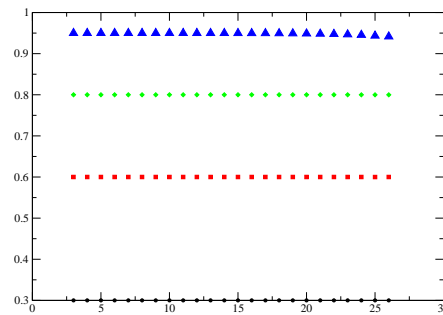
A new state, not seen before, is present in the spectrum close to the first excited state.

A toy model with 5 states in the spectrum to understand this fact:

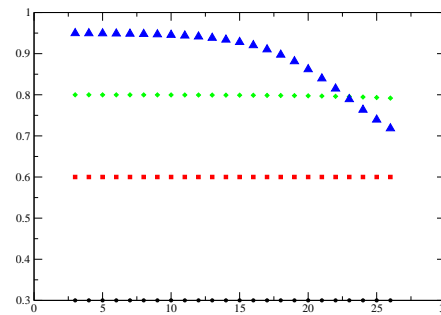
spectrum
0.3
0.6
0.63
0.8
0.95

$$\text{Matrix of couplings} = \begin{bmatrix} 0.6 & 0.25 & x \times 0.4 & 0.1 & 0.5 \\ 0.61 & 0.27 & x \times 0.39 & 0.11 & 0.51 \\ 0.58 & 0.24 & x \times 0.42 & 0.12 & 0.52 \\ 0.57 & 0.25 & x \times 0.41 & 0.1 & 0.49 \\ 0.56 & 0.26 & x \times 0.36 & 0.08 & 0.48 \end{bmatrix}$$

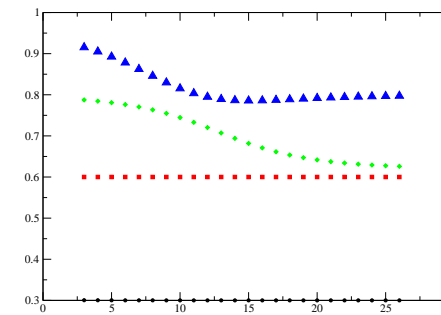
$x = 0.001$



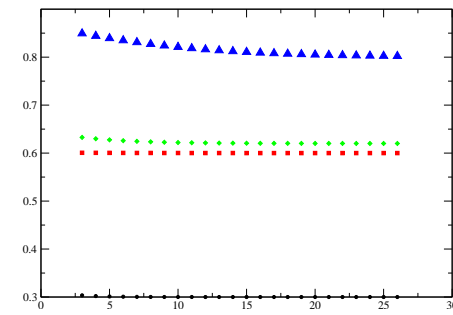
$x = 0.01$



$x = 0.1$



$x = 1$



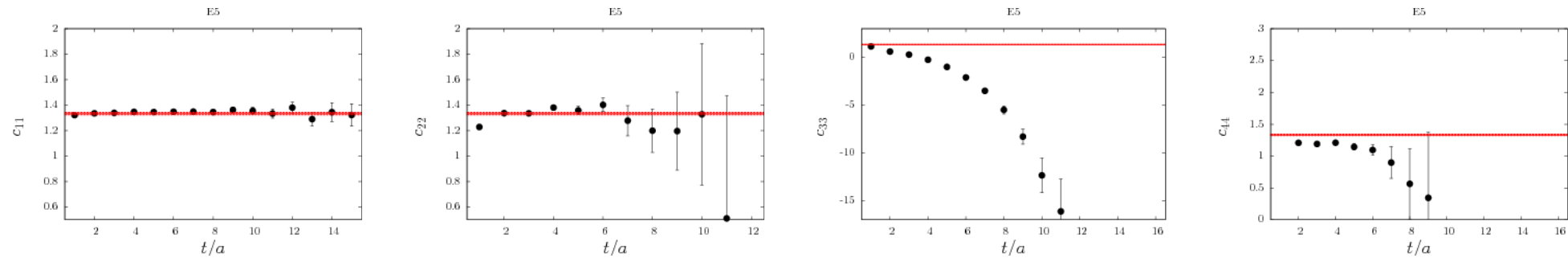
$x \ll 1$ : GEVP isolates states 1, 2, 4 and 5;  $x \rightarrow 1$ , GEVP isolates states 1, 2, 3 and 4

A GEVP can "miss" an intermediate state of the spectrum if, by accident, the coupling of the interpolating fields to that state is suppressed.

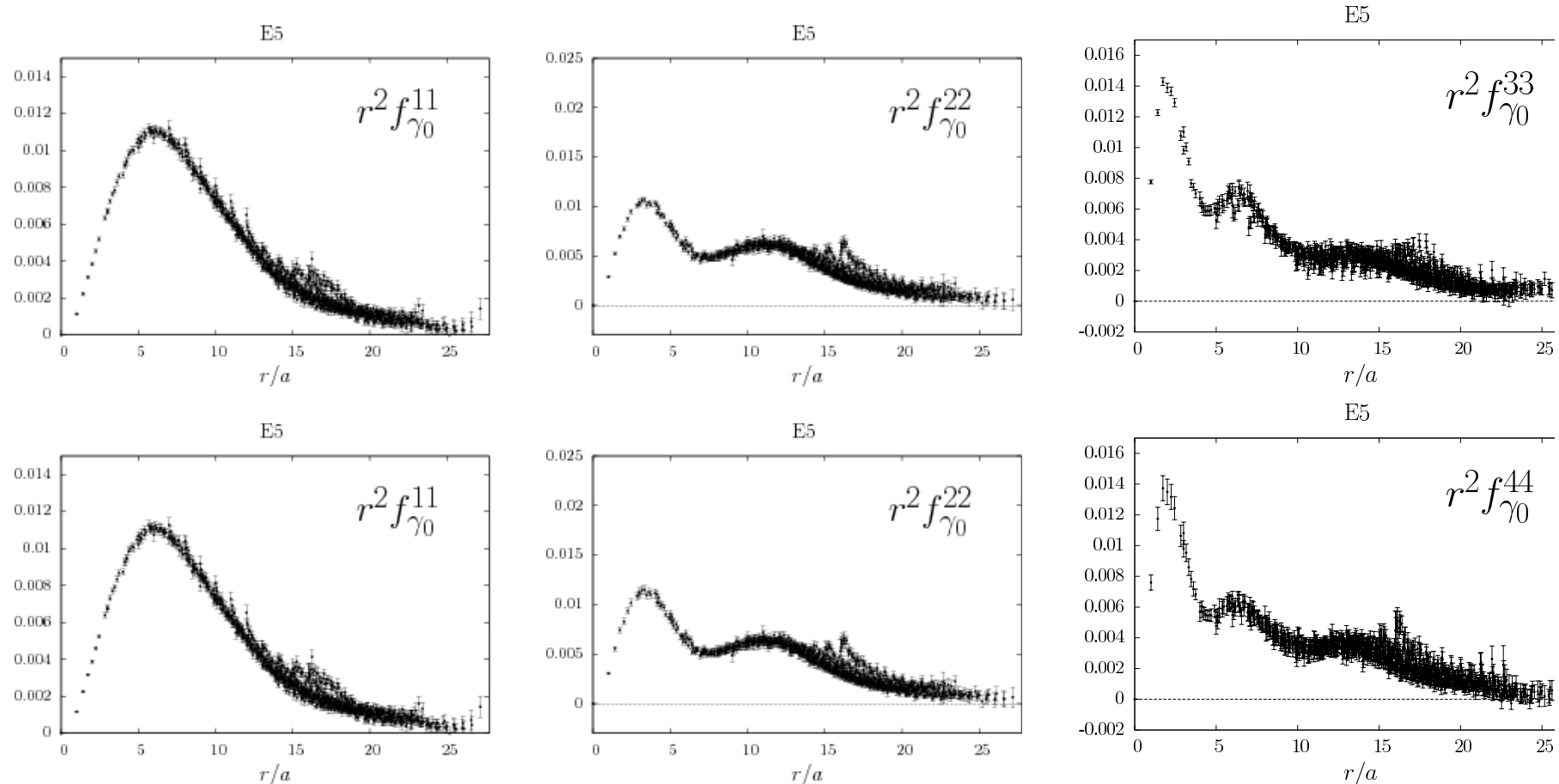
Our claim: using interpolating fields  $\bar{q}\gamma_k b$ , no chance to couple to multi-hadron states while inserting an operator  $\bar{q}\nabla_k b$  may isolate the  $B_1^*\pi$  two-particle state.

Clues come from density distributions obtained with that interpolating field, work is on-going to illustrate them.

Conservation of vector charge: not verified in the case of second excited state if the basis of interpolating fields incorporates  $\bar{q}\nabla_k b$ .



Including or not  $\bar{q}\nabla_k b$  does not change the profile of  $f_{\gamma_0}^{11}$  nor  $f_{\gamma_0}^{22}$ : it does in the case of  $f_{\gamma_0}^{33}$ .



## Outlook

- Excited meson states are massively produced in experiments. To exploit fruitfully the numerous data at Super Belle and LHCb, theorists do have to put an important effort in confronting their models predictions with measurements, by proposing to experimentalists unambiguous observables to look at.
- Parametrising the form factors  $f_+^{B(D) \rightarrow \pi}$  in the whole  $q^2$  region needs to compute the residues at the  $B(D)^*$ ,  $B(D)^*'$ , ... poles; a lattice measurement has been performed in the static limit of HQET to confirm the negative transition amplitude  $\langle B|A|B^*'\rangle$  as stated in phenomenology.
- Extract the density distribution of the  $B$  meson is beneficial to get the form factors at  $q^2 = 0$  associated to pionic couplings. Lattice computations allow a detailed comparison with quark models. Density distributions may be a check of the absence of any unwanted coupling between a given interpolating field of the  $B$  meson and a multihadronic state  $B\pi$ .